

EXPERIMENTAL AND COMPUTER SIMULATION STUDY OF RADIOACTIVITY OF MATERIALS IRRADIATED BY INTERMEDIATE ENERGY PROTONS

Yury E. Titarenko, Oleg V. Shvedov, Vyacheslav F. Batyaev, Evgeny I. Karpikhin,
Valery M. Zhivun, Ruslan D. Mulambetov

*Institute for Theoretical and Experimental Physics, B.Cheremushkinskaya 25,
117259 Moscow, Russia, e-mail: Yury.Titarenko@itep.ru*

Stepan G. Mashnik, Richard E. Prael, William B. Wilson
Los Alamos National Laboratory, Los Alamos, NM 87545, USA

August 28, 2018

ABSTRACT

The results of measurements and computer simulations of radioactivities and dose rates as functions of decay time are presented for ^{nat}Pb and ^{209}Bi irradiated by 1.5-GeV protons, ^{59}Co , ^{63}Cu , and ^{65}Cu irradiated by 0.13- and 1.2-GeV protons, and ^{232}Th and ^{nat}U irradiated by 0.1- and 0.8-GeV protons. The activities and dose rates are measured by direct high-precision γ -spectrometry. The irradiations were made using external beams extracted from the ITEP U-10 proton synchrotron. Simulations made using the LCS and CINDER'90 code systems are compared with measurements.

INTRODUCTION

The design of a hybrid system driven via a high current accelerator needs to have information about residual nuclides that are produced by high energy protons in the target and in constructional elements, defining a number of technical features of the system.

Our previous works [1,2] present the results of experimental measurements of residual radioactive nuclides produced in the target and constructional materials irradiated with 0.13- and 1.5-GeV protons. Predictive powers of a number of high energy codes were investigated using the experimental data. A general conclusion found insufficient accuracy of the codes to simulated radionuclide yields, both independent and cumulative, with the mean deviation of simulated results from experimental data often of a factor of 2 or higher. Reliable information on the yield of each residual nuclide is very important and such characteristic can be defined as “individual”.

Unlike our previous works, this study is aimed to investigate the predictive power of codes not for individual but for “integral” parameters – time dependent activation and dose-equivalent rate (called dose rate here-

after) which are directly dependent on summed yield of individual radionuclides. For such “integral” characteristics, one may expect a much better predictive power of codes than in simulations of “individual” parameters. We believe that the dose rate due to emanations of the γ -s from any hybrid system part being irradiated is one of the most important working parameters in applications.

Here, the LAHET [3] and HMCNP Monte Carlo transport codes were used together with the code CINDER'90 [4] to simulate the build-up and decay of the products.

EXPERIMENT

The irradiations of experimental samples were carried out using external beams of the ITEP proton synchrotron. A sandwich of experimental and aluminum samples of the same diameters of 10.5 mm was placed perpendicularly to the proton beam during each irradiation. The parameters of irradiations and of experimental samples are presented in Table 1.

The CANBERRA spectrometer based on the GC-2518 Ge detector was used to measure γ -spectra of irradiated experimental and aluminum samples. γ -spectra processing and nuclide identification were made using the ASPRO and SIGMA codes and the PCNUDAT nuclear database. ^{24}Na formation in aluminum samples was used to determine the irradiation time integrated proton flux. The details of irradiation techniques, schemes and parameters of external beams, techniques of nuclides identification and their cross section determination can be found in [1].

SIMULATION TECHNIQUE

The simulation of build-up during irradiations and following decay of produced nuclides was made using the LCS [3] and CINDER'90 [4] code systems.

Table 1: Parameters of irradiations and experimental samples

N	Target	Parameter			
		Sample weight (mg)	Proton energy (MeV)	Irradiation time (min)	Proton flux (p/cm ²) during irradiation
A	^{nat} Pb	143.8	1478	15	2.43E+13
B	²⁰⁹ Bi	368.05	1478	15	2.67E+13
C	⁵⁹ Co	202.7	1186	45	6.86E+13
D	⁵⁹ Co	196.6	127	60	2.29E+13
E	⁶³ Cu	80.2	1186	70	1.08E+14
F	⁶⁵ Cu	92.6	1186	70	1.37E+14
G	⁶³ Cu	425.55	127	9	1.56E+11
H	⁶⁵ Cu	521.6	127	9	1.49E+11
I	²³² Th	87.5	97	40	6.31E+12
J	²³² Th	89.6	795	30	4.86E+12
K	^{nat} U	159.2	97	60	9.22E+12
L	^{nat} U	160.9	795	60	7.43E+13

LCS includes the LAHET and HMCNP Monte-Carlo radiation transport codes. LAHET follows protons of all energies and secondary neutrons above 20 MeV throughout the geometry using a selection of on-line nuclear models and parameters; for these calculations LAHET2.83 was used with default selections except for use of ISABEL intranuclear-cascade model with default parameters, preequilibrium model following intranuclear cascade, and nuclear elastic scattering for neutrons and protons.

LAHET passes the position, direction, and energy of all neutrons below 20 MeV as source particles to HMCNP, which uses evaluated cross-section data to follow all neutrons (and photons, if desired) throughout the geometry.

The regional nuclide production (At./proton) from LAHET and the binned neutron fluence (n/bin-p-cm²) from HMCNP are scaled by region volume (cm³) and proton source strength (p/s) to form production probabilities (At./cm³-s) and neutron fluxes (n/cm²-s). These are used with evaluated cross sections and decay data in CINDER'90 to calculate the temporal nuclide inventory during and following irradiation.

In these simulations of thin-target measurements in environment having no features contributing to lower-energy neutron flux, contributions to nuclide inventory from the lower energy neutron reactions in HMCNP and in CINDER'90, although included, are negligible.

To investigate the real predictive power of the codes but not just an ability to describe some known measured data, all simulations have been performed at Los

Alamos strictly before receiving any experimental data from Moscow that could be compared with theoretical results.

PROCESSING EXPERIMENTAL AND SIMULATED DATA

Determination of experimental activities and dose rates

Activity of each nuclide in experimental samples was calculated via least square approximating nuclide counting rates of corresponding γ -energy peaks taking into account γ -yields and absolute effectiveness of the spectrometer at corresponding γ -energy. The total activities of the targets were defined as a sum of activities of individual nuclides. The individual activities were determined dependently of properties of precursors present for practically all measured products:

1) If precursors are absent or have lifetimes that are either much less than the first measurement time after irradiation or much higher than the last measurement time, the following formula was used for activity calculation:

$$a(t, T) = \frac{A_0}{\varepsilon\eta} \exp[-\lambda(t - T)] .$$

2) If precursors have lifetimes that are comparable with times passed after irradiation, the following formula was used:

$$a(t, T) = \frac{1}{\varepsilon\eta} \{A_1 \exp[-\lambda_1(t - T)] + A_2 \exp[-\lambda_2(t - T)]\} ,$$

where, A_0 , A_1 , and A_2 are the coefficients determined via the least square approximation; λ , λ_1 , and λ_2 are the decay constants of the nuclide and its precursors; t is the time after starting the irradiation; T is the irradiation duration; η is the γ -yield; ε is the absolute effectiveness of the spectrometer.

The dose rate at 1 cm distance from a target was defined via summing individual nuclides dose rates which were determined via individual activities multiplied by K_γ -dose coefficients calculated for each nuclide using methods and data described in [5].

Simulated activities and dose rates

To have a correct comparison of obtained experimental results with the simulated ones, the simulated total activities were calculated by summing the individual simulated activities of only the nuclides that were identified in measurements and used for calculating experimental activities. The simulated dose rates were calculated by summing the individual dose rates of the same nuclides.

AGREEMENT BETWEEN SIMULATED AND EXPERIMENTAL RESULTS

The determined experimental and simulated activities are presented in Figures 1–6. Additionally, the figures show the mean squared deviation factors calculated via

$$\langle F \rangle = 10 \sqrt{\left\langle \left(\lg \left(\frac{\text{theor. value}}{\text{exp. value}} \right) \right)^2 \right\rangle}$$

for each of the data sets compared, where $\langle \dots \rangle$ designates averaging over all of the comparison events.

As seen from the figures, the simulated results are in good agreement with experimental data for most of the targets. In most cases, the mean squared deviation factor is from 1.15 to 1.47. The following variations of simulated-to-experimental agreements along time range are observed:

1. ^{nat}Pb and ^{209}Bi : the simulated activities during the first 15 hours after irradiation are on the average underestimated by a factor of 2, meanwhile, the results are in a much better agreement later.
2. ^{63}Cu , $E_p = 1186$ MeV: the simulated results, both for activity and dose rate, are in average 3 times underestimated during the first 5-300 hours after irradiation, meanwhile the discrepancies are negligible for other times.
3. ^{63}Cu and ^{65}Cu , $E_p = 127$ MeV: the simulated results, both of activity and dose rate, are in average 1.5 times lower for ^{63}Cu , and 2 times underestimated for ^{65}Cu after ~ 1 day after irradiation, meanwhile during the first day after irradiation the results either practically coincide with experimental data (^{63}Cu) or lie very close to them (^{65}Cu).

The largest discrepancy between simulated and experimental data is observed for ^{59}Co irradiated with 127 MeV protons. Simulated activities are about 4 times, and dose rates – 2 times underestimated almost for the entire range of time. This reflects, probably, the importance of nuclear structure effects for this reaction (relatively low bombarding energy and vicinity of the target ^{59}Co to the doubly magic ^{56}Ni and magic ^{57}Ni nuclides) and an inadequate capability of LAHET to describe nuclide production near closed shells, which could be a result of using not good enough approximations for level densities, for inverse cross sections of evaporated and preequilibrium particles, and/or, for nuclear masses and binding energies near closed shells.

CONCLUSIONS

As a whole, the simulated activities and dose rates are in good agreement with experimental data for most

of the targets along the whole time range. Nevertheless, some serious discrepancies at certain times after irradiation, especially for ^{59}Co , were obtained.

At the moment, we have not made a detailed investigation of the causes of the observed discrepancies. The list of products that are produced in the irradiations and/or are observed at decay phase and much contributes to the discrepancies observed have not been defined yet. Also, the contribution of various modes of nuclides formation in nuclear interactions (spallation, fission, fragmentation) to the observed discrepancies has not been analyzed properly.

This work is our first step in the study of experimental and simulated activities of targets induced by intermediate and high energy protons. The analysis of observed discrepancies will be continued, and, if possible, will be extended to thick targets in which secondary neutrons, rather than the incident protons, have the largest contribution to target activation. The use of the ISABEL model in LAHET for the higher-energy simulations above its nominal 1-GeV limit could lead to inconsistencies; similar calculations using the alternate Bertini model, or preferably the nuclear models of the CEM95 code [6], in LAHET are called for.

The experimental part of this work have been supported by the ISTC Project #839 and the theoretical study was supported by the U. S. Department of Energy under contract W-7405-Eng-36.

REFERENCES

1. Yu. E. Titarenko et al., *Nucl. Instr. and Meth. A* 414, 73 (1998).
2. Yu. E. Titarenko et al., *Proc. Second Int. Topical Meeting on Nuclear Applications of Accelerator Technology (AccApp'98)*, Gatlinburg, TN, USA, September 20-23, 1998, pp. 164-171 and references therein.
3. R. E. Prael and H. Lichtenstein, "User guide to LCS: The LAHET Code System," Los Alamos National Laboratory Report LA-UR-89-3014 (1989).
4. W. B. Wilson, T. R. England, and K. A. Van Riper, "Status of CINDER'90 Codes and Data," *Proc. Fourth Workshop on Simulating Accelerator Radiation Environments (SARE4)*, Knoxville, TN, USA, September 14-16, 1998, p. 69.
5. N. G. Gusev, V. P. Mashkovich, G. V. Obvintsev, "Gamma Irradiation of Radioactive Isotopes and Fission Products," Moscow (1958) [in Russian].
6. S. G. Mashnik, "User Manual for the Code CEM95", JINR, Dubna, 1995; <http://www.nea.fr/abs/html/iaea1247.html>.

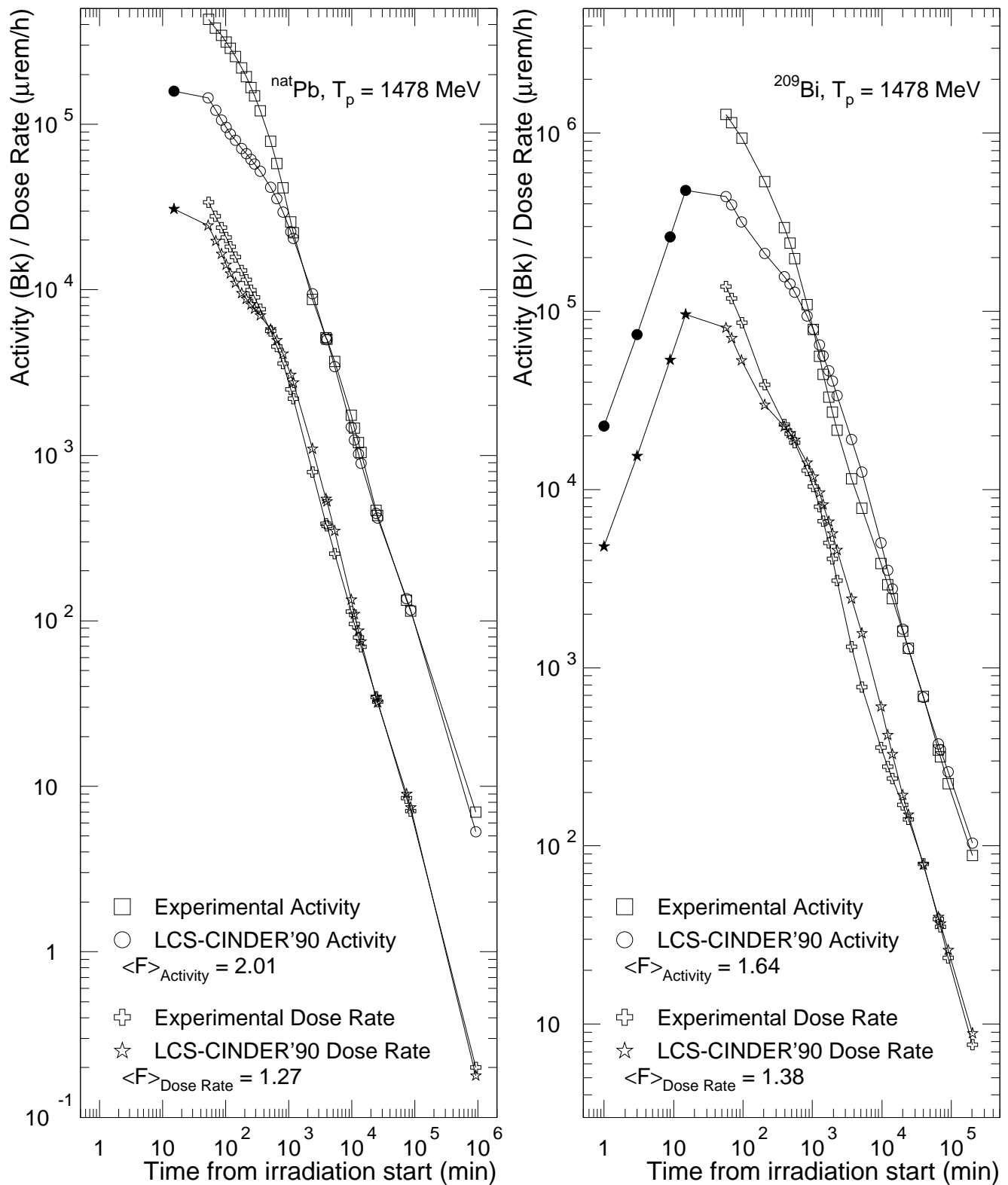


Figure 1: Experimental activities and dose rates and results calculated with the LCS-CINDER code system for ^{nat}Pb and ^{209}Bi irradiated with 1478 MeV protons. The filled symbols show calculated values during the irradiation. The mean squared deviation factors (see text) are shown for both.

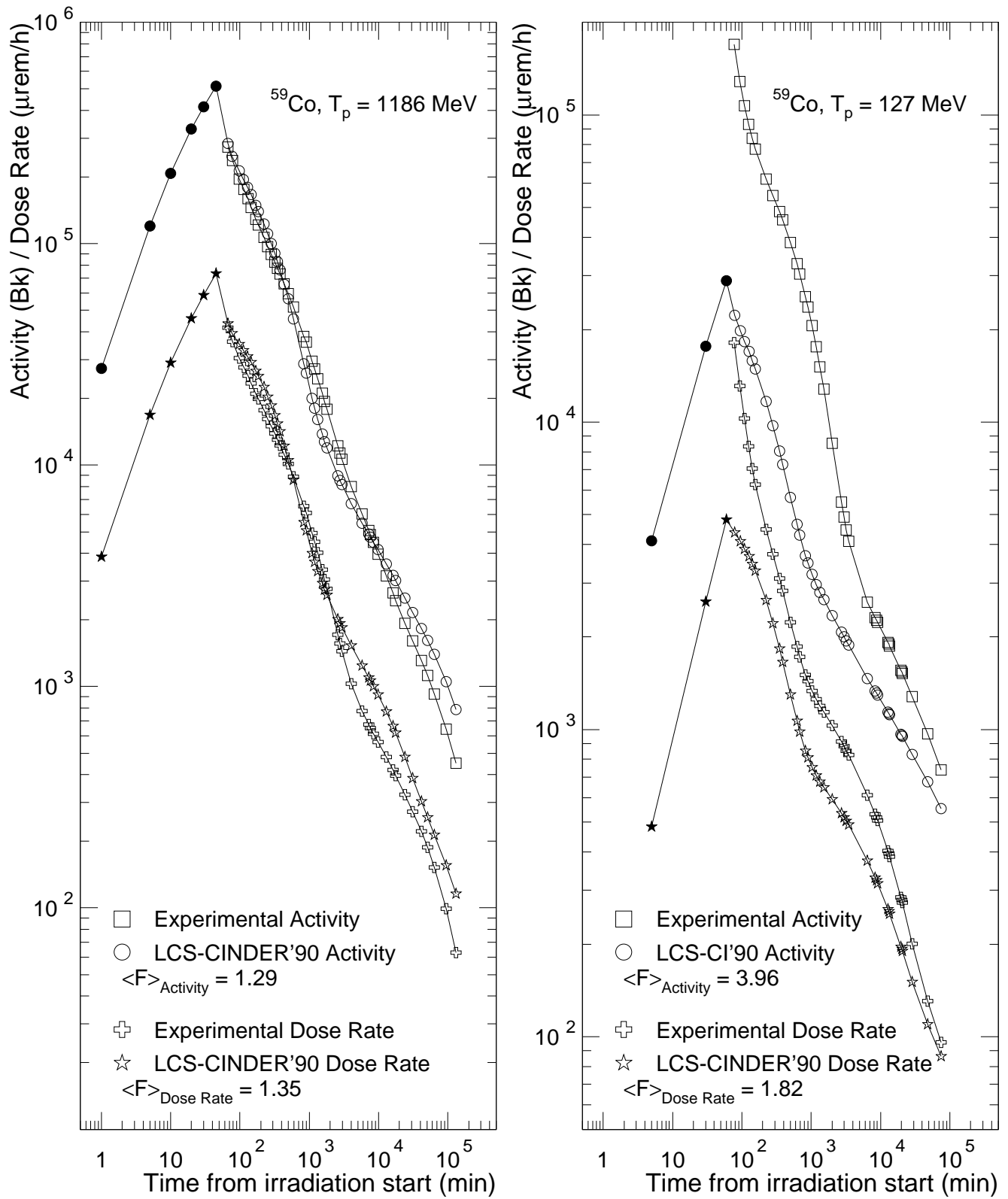


Figure 2: The same as Fig. 1, but for ^{59}Co irradiated with 1186 MeV and 127 MeV protons.

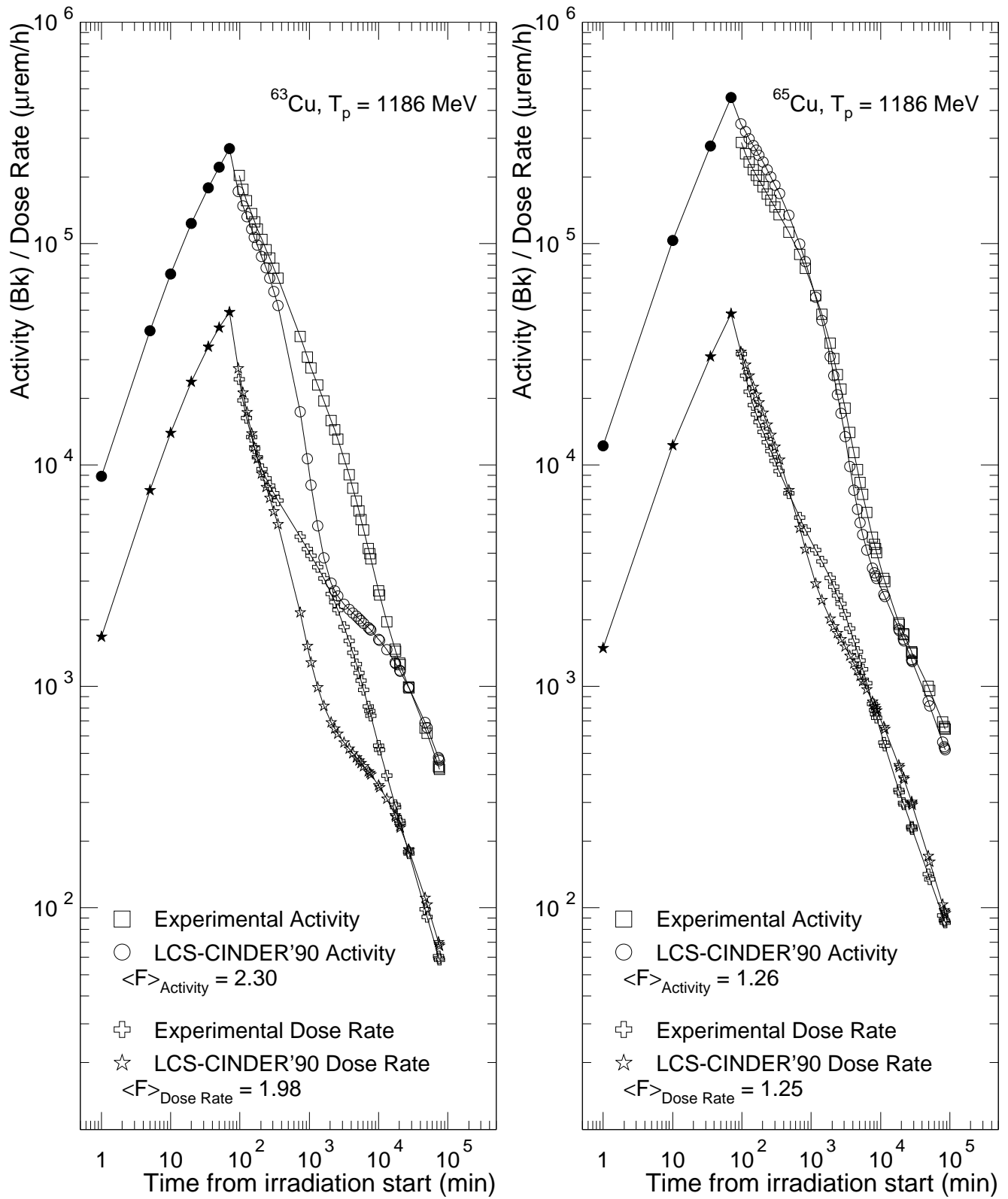


Figure 3: The same as Fig. 1, but for ^{63}Co and ^{65}Co irradiated with 1186 MeV protons.

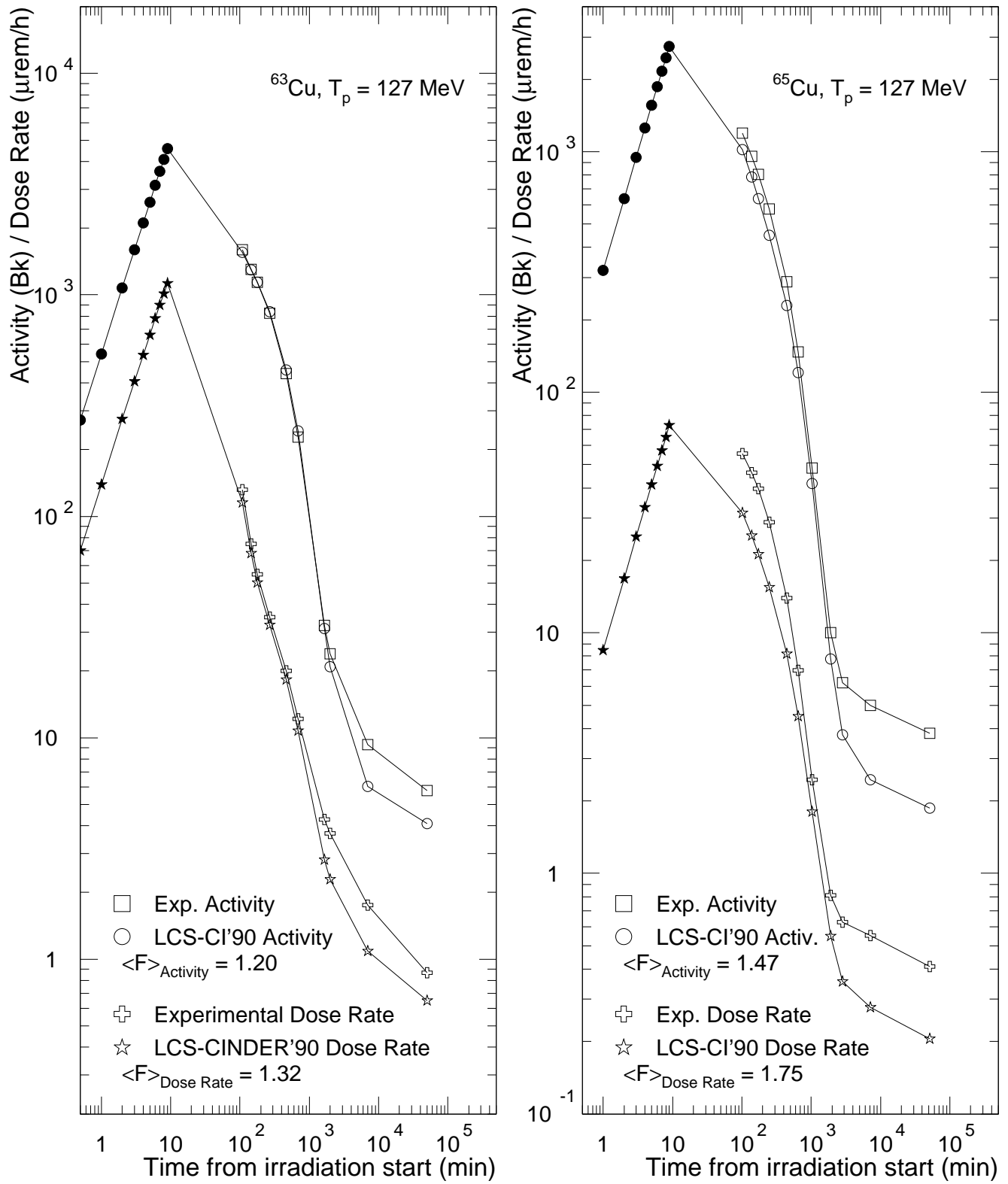


Figure 4: The same as Fig. 1, but for ^{63}Co and ^{65}Co irradiated with 127 MeV protons.

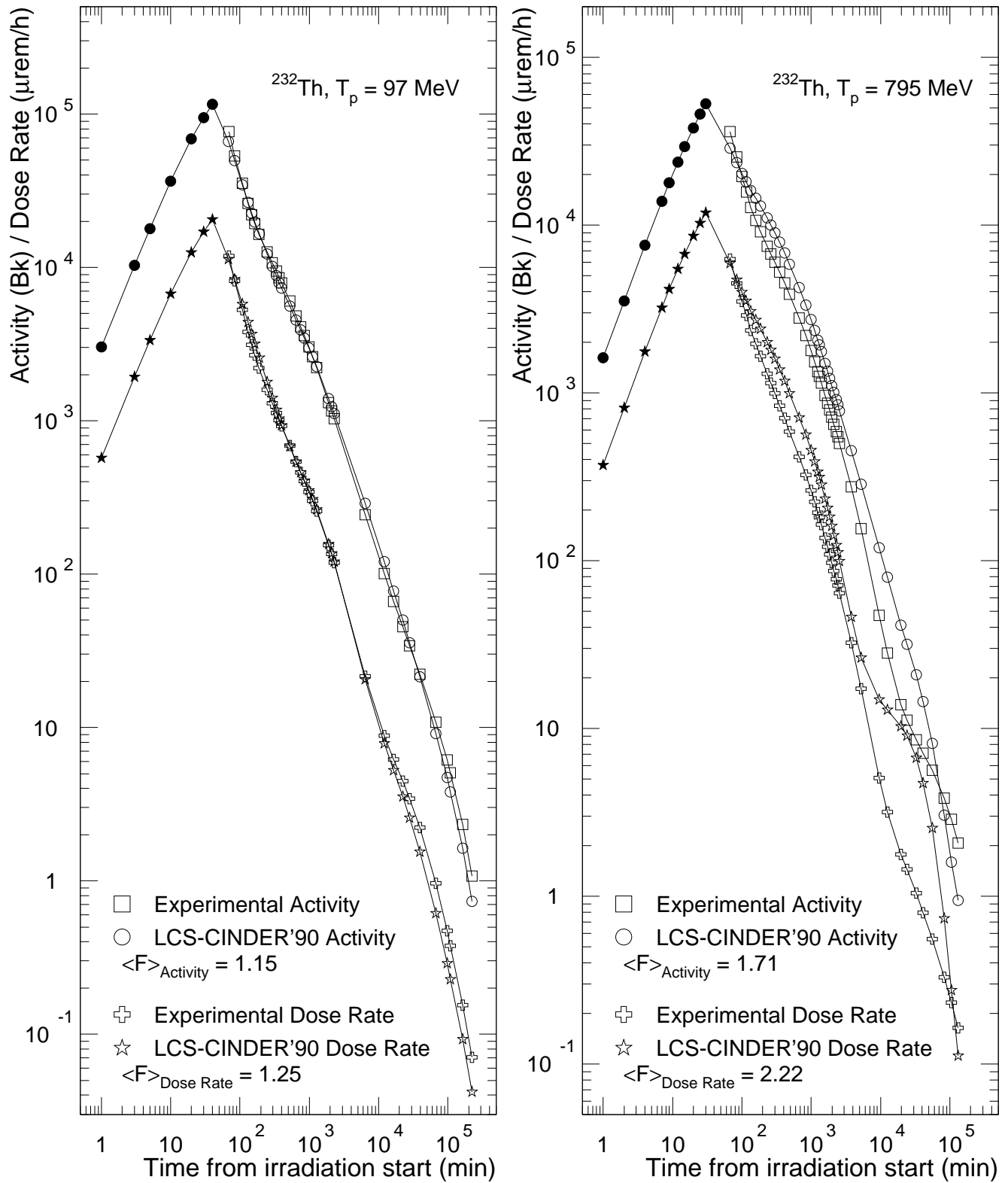


Figure 5: The same as Fig. 1, but for ^{232}Th irradiated with 97 MeV and 795 MeV protons.

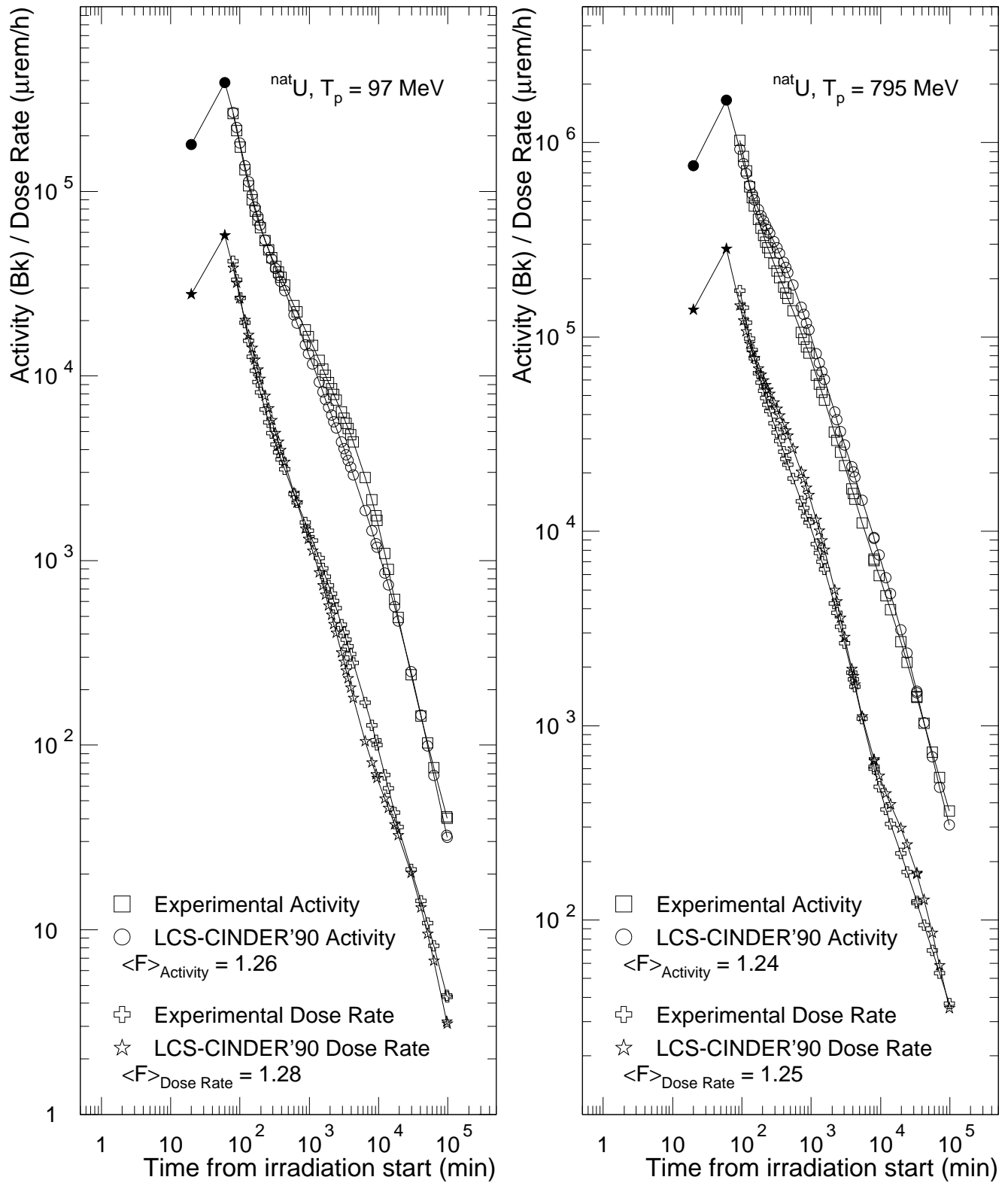


Figure 6: The same as Fig. 1, but for ^{nat}U irradiated with 97 MeV and 795 MeV protons.